Euro. Jnl of Applied Mathematics (2016), *vol.* 27, *pp.* 357–376.
doi:10.1017/S0956792515000388

Modelling insurgent attack dynamics across geographic scales and in cyberspace †

N. F. JOHNSON[1], D. E. JOHNSON[2] and E. M. RESTREPO[3]

[1]*Department of Physics, University of Miami, Coral Gables, FL 33124, USA*
email: *njohnson@physics.miami.edu*
[2]*Department of Government, Harvard University, Cambridge, MA 02138, USA*
email: *danielajohnsonrestrepo@college.harvard.edu*
[3]*Department of Geography, University of Miami, Coral Gables, FL 33124, USA*
email: *e.restrepo@miami.edu*

(*Received 5 January 2015; revised 23 May 2015; accepted 22 June 2015; first published online 21 July 2015*)

We discuss the emergence of common mathematical patterns governing the timing and severity of insurgent and terrorist attacks, across geographic scales and including cyberspace. We present mathematical models that provide a generative explanation of these patterns. Despite wide variations in the underlying settings and circumstances, the ubiquity of these patterns suggests there is a common way in which groups of humans fight each other. Our empirical findings follow from the analysis of myriad state-of-the-art datasets with resolution at the level of individual attacks, while our mathematical modelling involves numerical and analytical solutions of fission–fusion dynamics together with progress curve analysis.

Key words: Modelling and interdisciplinarity; Behavioural and social sciences; Applications in sciences

1 Introduction

Attacks by insurgents and terrorists are, almost by design, supposed to surprise their enemy and impact public opinion. Surprise is a particularly important tool since insurgent and terrorist organizations are typically much smaller and weaker than the state that they want to attack, hence they would likely experience heavy losses if they were to confront their opponent in any open or obvious way. This feature, coupled with the wide diversity of possible conflict terrains, conditions and causes, makes it counter-intuitive to expect attacks to follow any common pattern. Indeed typical time-series of attacks look completely random to the eye. As we show in this paper, however, universal patterns do emerge.

The statistical analysis of conflict data – in particular through body counts – dates back one hundred years to Richardson [1]. Trained as a physicist, Richardson analysed compilations of casualty data across many different wars [1]. Around the same time, mathematical modelling of the underlying conflict dynamics began to be developed by Lanchester and others, based on mass-action differential equations [2]. However, both

† NFJ gratefully acknowledges a grant from the Office of Naval Research (ONR): N000141110451.

these studies suffered from a lack of availability of spatiotemporal data concerning individual attacks on a daily scale, thereby putting beyond reach any rigorous mathematical modelling of the event-level fluctuations within a given conflict or terrorist campaign. Though estimates might have been known for entire conflicts (e.g. World War II) or specific battles, the fluctuations across day-to-day skirmishes were not. This situation has recently changed, however, due to the explosion in conflict coverage by the media and Non-Government Organizations together with academic projects aimed at logging event-level casualties at the highest possible resolution.

This paper uses generative mathematical models to interpret certain statistical patterns observed in insurgent, terrorist and cyber-attacks across different geographic settings including cyberspace. Both the mathematical modelling and the empirical statistical analysis draw on approaches used within the physics community [3–10]. They complement the exciting hotspotting approaches recently developed in the mathematical criminology field [12–15], which have also been applied to insurgency dynamics [12, 13]. They are also consistent with recent developments in the social science and complex systems literature [16–43]. The empirical results cross a wide range of geographical scales – from municipalities up to entire continents across the globe, and with great diversity in terms of terrain, underlying cause, socioeconomic and political setting, cultural and technological background. Casualty data are drawn from all available sources, including academia, non-government organizations and official government records. The following steps summarize our methodology: (i) Identify systematic behaviours in the ongoing timelines of attacks within a given insurgent conflict or terrorist campaign. (ii) Quantify the resulting stylized statistical facts. (iii) Develop generative mathematical models of the underlying dynamics which are minimal and yet which are able to reproduce these observed statistical features.

The broader implication of our findings is that irrespective of the underlying circumstances and locations, groups of humans tend to "do" insurgency and terrorism in a surprisingly generic way across different geographic scales, including cyberspace. Hence, this work provides a link to the universality uncovered in non-violent human group activities including traffic and stock market trading [27, 44, 45]. The results, narrative and discussions in this paper draw heavily on Refs. [28, 29, 46, 47].

2 Background

Within a given insurgent conflict, terrorist or cyber campaign, the observable output from an attack at time t can in principle be represented as a vector $\mathbf{x}_i(t)$ whose elements might describe the number of casualties for each population type at place i, and the different weapon types used. In line with military nomenclature, we refer to the insurgent, terrorist or cyber-attacking population as Red, even though they may be a heterogeneous collection of fighters, and we refer to the state (e.g. coalition military or security force) as Blue. Non-participating civilians are referred to as Green.

Our data sources are a mix of real-time media databases, official (government and non-governmental organization) reports and academic studies [47]. For the insurgent conflicts, our sources include the Uppsala Conflict Data Program, icasualties.org, Marc Herold of the University of New Hampshire and the ITERATE terrorism database. Our Iraq data also amalgamates three separate data sets: Iraq Body Count, ITERATE

https://doi.org/10.1017/S0956792515000388 Published online by Cambridge University Press

and icasualities.org. Sierra Leone data comes from Macartan Humphreys of Columbia University. Malcolm Sutton is the source of the data for the Northern Ireland conflict, having himself built on a large number of sources. Data for the Peruvian conflict derives from the Truth and Reconciliation Committee. The Colombian Conflict Database was provided kindly by the Conflict Analysis Resource Center [48]. The Spanish and American civil war data came from the work of Ron Francisco at the University of Kansas. Comparative results for sexual violence against women come from Ref. [49] while suicides, accidents, homicides etc. were obtained from analysing the data of Medicina Legal in Colombia. In terms of terminology, we adopt the language in which a cell is a cluster of a few Red agents (e.g. insurgents) which carries out a given attack, and organization is the entire Red outfit – even though we stress that we do not want to assign any specific organizational capabilities, or assume that Red is necessarily well organized, or following a hierarchy. Indeed, as we will show, one of the implications of our work is that the cells are loose and transient in terms of their operational activity. This is likely why they are so hard to track.

To date, the mathematical models of human conflict that have been proposed in the literature tend to resemble predator-prey models which themselves are akin to a chemical reaction between two reagents, e.g. Red and Blue. These models' dynamics are usually evaluated in the form of continuous differential equations in order to obtain partially analytic results, or through computationally intensive cellular automata or individual-based models on some kind of fixed grid such as a static spatial network or checker-board [50, 51]. Beyond the few-particle limit, mean-field mass action equations including Lotka–Volterra can provide reasonable qualitative descriptions of the average behaviour, i.e. $dN_R(t)/dt = f(N_R(t), N_B(t))$ and $dN_B(t)/dt = g(N_R(t), N_B(t))$, where $N_R(t)$ and $N_B(t)$ are the Red and Blue population's strength at time t. However, actual insurgent conflicts and terrorist campaigns feature a number of complications that challenge such mathematical models. In particular, the following features arise, each of which is addressed in the mathematical models that we present in subsequent sections: (1) The classic image of a battle being fought between two well-regimented armies lining up at dawn on opposite sides of a field or plain, does not describe the fragmented, fluid situation of modern insurgencies [16–18], either in the real or cyber worlds. Instead, Red is likely to show significant intra-population group (e.g. cluster) formation which can change unexpectedly over time as in the animal world [24]. Though it is possible to generalize mass-action predator-prey equations to mimic such dynamical grouping effects, such generalizations present a dilemma of how to choose an appropriate functional response term for $f(N_R(t), N_B(t))$ and $g(N_R(t), N_B(t))$. (2) Broadcasting communications now exist in which events and images can be portrayed almost instantly to a broad sector of the global population, enabling Red to almost instantaneously learn what has, and is, happening locally, nationally and internationally and hence adapt quickly. (3) Personal media resources such as Facebook and Twitter, together with emails and texts, mean that fighters (and potential fighters) who are separated across different streets, or towns, or countries, or continents, can be connected together within a second – and hence they can coordinate their actions such that they begin to behave as one quasi-coherent group (or "cell"), even though they may never have met each other and may even be geographically located on separate continents. As a corollary, the members of such a cell – who may not

be physically connected, but whose actions are somehow coordinated through the use of technology – may suddenly lose their collective coherence (e.g. loss of communications, or loss of trust) meaning that the cell has effectively fragmented abruptly. At the press of a button on a cellphone keyboard or touch of a keystroke, they instantaneously disappear into the background noise generated by everyday human activities. Given this, the vision that we adopt of the complex interactions within Red, and between Red, Blue and Green is that of a complex ecology whose dynamics and internal interactions may change and adapt over time, with adaptation–counter-adaptation and communication via some underlying dynamical network. This view is in accordance with the state-of-the-art view of modern violent gangs proposed by Felson [52], and the descriptions of insurgencies by Kilcullen, Robb and Kenney [16–18]. Our mechanistic approach is also remarkably consistent with current thinking in the social sciences – in particular, analytical sociology as developed by Hedstrom [53].

3 Attack severity: Coalescence–fragmentation model

Our analysis across datasets for different conflicts reveals no evidence for a strong systematic correlation between the severity of fatal events and their timing. This is consistent with reports from other researchers [8] and means that we can analyse the severity of fatal events separately from their timing. As a result, we have found that the event severity distribution is essentially stationary throughout the main portion of each conflict, while the timing of individual events is a non-stationary process with periods of initial escalation or de-escalation. We therefore analyse severity by aggregating all events across the main portion of each conflict, checking that the choice of window does not affect our conclusions. Given the ubiquity of power-law forms in other complex systems involving human collective activity, we focus on analysing the extent to which power-laws provide a good fit to the tail of the severity distribution.

The events listed in most databases of insurgent conflicts comprise primarily civilian casualties (i.e. Green) that were inflicted by Red – irrespective of whether the underlying event was an attack by Red on Blue, or an attack by Red on Green to force them to cooperate, for example. Furthermore, the nature of insurgent war means that the number of civilian casualties is typically far larger than that of Red or Blue. Empirically, it should therefore make little difference if one analyses just Green casualties inflicted by Red, or Green and Blue combined. We have checked that this is indeed the case for our results in Figure 1 where the distinction is known. To simplify our explanatory mathematical model for the results in Figure 1, we therefore regard the casualties in each event as representing an imprint of the strength of the Red cell that is involved in the event. When it comes to the event timing, most events are actually attacks initiated by Red directly against Blue – or directly against Green, which in turn means against Blue since it is Blue who are supposed to protect Green. Red, Blue and even Green will in general adapt and counter-adapt to differing degrees and in different ways over time to initiate or prevent Red's next attack, however this becomes too complex to analyse without detailed information about each side's daily activities. Hence, we will discuss the timing of attacks (Section 4) in terms of an ongoing struggle between Red and Blue's adaptation and counter-adaptation. In essence, we therefore assume that Green is a passive entity that has no dynamics itself

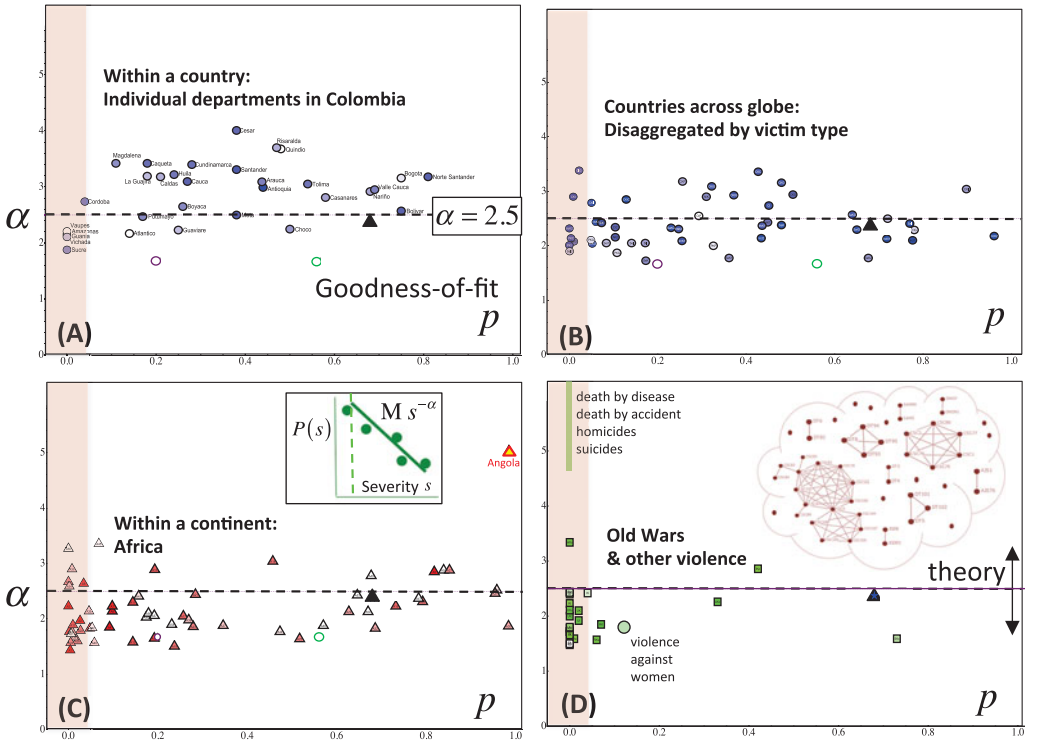

FIGURE 1. (A) Results of power-law fitting procedure for the tail of the distribution for the severity (i.e. number of casualties) per event (attack). See inset in (C). Each data-point shows the best-fit α value and the goodness-of-fit parameter p for the distribution of events (attacks) occurring in a particular department during Colombia's ongoing narco-guerilla war. The state-of-the-art fitting procedure is described and referenced in Ref. [47]. (B) Results for high-profile modern conflicts across the world, including Iraq. (C) Results for countries across a given continent (Africa). (D) Comparative results for conventional wars and other forms of human violence. Inset shows Provisional Irish Republican Army (PIRA)'s operational network in South Armagh [47]. The theoretical value $\alpha = 2.5$ which is shown by dashed horizontal line, emerges from the vanilla version of our theory derived in the text. Purple ring shows value for all interstate wars from 1860–1980. Green ring is value for entire Africa database. Black triangle shows value for global terrorism attacks. A goodness-of-fit less than 0.05 implies that it is unlikely that the data have a power-law tail (see red-shaded area). One-sided struggles such as natural deaths and suicides, do not show the power-law tail pattern. The darker the colour of each data-point, the larger the total number of victims (i.e. more total casualties). Data drawn and adapted from Ref. [47].

either in terms of grouping or strategy and instead simply soaks up the impact of the attacking Red. We must wait for data to become available in the future concerning what precisely Red, Blue and Green are doing on the daily scale in the lead-up to each event, in order to go beyond this approximation.

Figure 1 summarizes our findings for the severity distribution from applying a state-of-the-art maximum likelihood fitting procedure for a power-law $s^{-\alpha}$ to the tail in the distribution of the severity of individual events within a given conflict; s is the severity of an individual event which, in the case of violent conflict, is the number killed or

https://doi.org/10.1017/S0956792515000388 Published online by Cambridge University Press

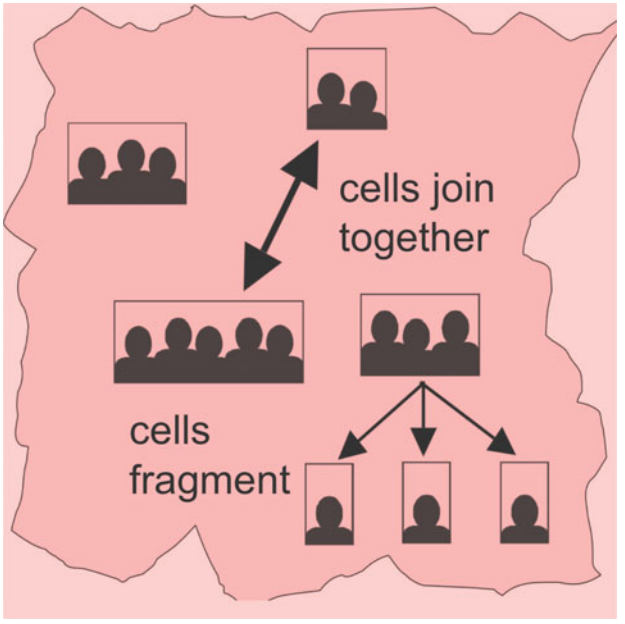

FIGURE 2. Illustration of the dynamical grouping featured in our model of Red (i.e. coalescence–fragmentation dynamics). Each Red cell has a strength (i.e. insurgent members, equipment, information) representing the typical number of people that the cell will kill in an attack. Red has overall strength N which we take for simplicity as a constant, distributed into dynamically evolving cells with time-varying size, number and composition. In the illustration, the strength is represented by the number of shadows (i.e. number of people that cell will likely kill in an attack). Total number of cells $N_g(t)$ varies with time such that $N_g(t) \geqslant 1$ (i.e. the smallest number of cells is when every object belongs to this same cell) and $N_g(t) \leqslant N$ (i.e. the largest number of cells is when every object is isolated). In this illustration, the number of cells of a given size s at this timestep t, prior to fragmentation of the cell of size 3 into 3 cells of size 1, is $n_{s=1}(t) = 0$, $n_{s=2}(t) = 1$, $n_{s=3}(t) = 2$, $n_{s=4}(t) = 0$, $n_{s=5}(t) = 1$, $n_{s\geqslant 6}(t) = 0$. The total number of insurgents is $N = \sum_s n_s(t) = 1 \times 2 + 2 \times 3 + 1 \times 5 = 13$. The number of cells $N_g(t) = 4$. Following fragmentation, $N = 13$ but $N_g(t) = 6$.

injured in an attack; α is the power-law exponent; p is the goodness-of-fit; M is the normalizing factor. Most of the severity distributions from insurgent conflicts and terrorism in Figure 1, approximate to a power law and have a corresponding power-law exponent around 2.5.

Our explanatory model of this 2.5 power-law result is shown schematically in Figure 2. Here, we motivate its mechanisms and then solve analytically its most basic version, noting that we have shown numerically that the 2.5 value is remarkably robust to generalizations [33]. It builds on two key mechanisms within Red: Coalescence and fragmentation. The coalescence process mimics the situation in which two Red cells, or individuals in these cells, initiate a communications link between them of arbitrary range, for example a mobile phone call. The two cells therefore tend to coordinate their actions from then on. Indeed, the individual agents need not know each other, or be physically present in the same place. The long-range nature of the coupling makes it a reasonable description for physical insurgencies using modern communications in real space, as well as cells acting in cyberspace – or any mix of the two [18]. Indeed, the language of what

https://doi.org/10.1017/S0956792515000388 Published online by Cambridge University Press

is a cell and what is a group becomes irrelevant since the mechanistic operational details are now very similar. The fragmentation process may arise for a number of social or situational reasons, from breakdown in trust within a Red cell [16] through to detection of imminent danger by a Red cell [18,24]. It is well documented that groups of objects (e.g. animals, people) may suddenly scatter in all directions (i.e. complete fragmentation) when its members sense danger, simply out of fear [24] or in order to confuse a predator [24]. Or they may fragment following a clash in which the cell perceives that it is losing. The precise details of these mechanisms do not matter since they tend to give similar empirical distributions. The interactions in our model are distance-independent as in Ref. [5], since we are interested in systems where messages can be transmitted over arbitrary distances and hence mimic modern human communications. We stress that these mechanisms are consistent with observed animal anti-predator behaviours [11,24] and also those of criminal gangs [16,18,52]. The resulting coalescence–fragmentation process is consistent with observations of insurgent and terrorist structures as fragmented, transient and evolving [17,19]. As Gambetta states: [16] "... contrary to widespread belief, criminal groups are unstable." Further support is provided by Kenney's narrative [18]: "To protect themselves from the police, trafficking enterprises often compartment their participants into loosely coupled networks and limit communication between nodes"; "Trafficking networks . . . are light on their feet. They are smaller and organizationally flatter"; "In progressive-era New York, according to historian Alan Block, cocaine trafficking was organized by different networks of criminal entrepreneurs who formed, reformed, split, and came together again as opportunity arose and when they were able"; "loose collection of cells containing relatively small number of cell workers"; "Abu Sayyaf . . operates as a decentralized network of loosely coupled groups that conduct bombings, kidnappings, assassinations and other acts of political violence in pursuit of a common goal . . ". Kenney also highlights the close connection of traffickers to terrorists: "Al Qaeda share numerous similarities with drug-trafficking enterprises" [18]. The inset in Figure 1(D) for the Provisional Irish Republican Army shows further support, since it shows a similarly decentralized, clustered structure consistent with jihadist operational networks and other covert networks such as online gold farmers [47]. We note that in both the empirical Provisional Irish Republican Army network and our model, a link simply denotes some coordinated activity, but is not necessarily related to spatial proximity or acquaintance.

The above empirical observations suggest that the internal coherence of a Red population of strength N (equivalent to N agents) should be represented as a dynamically evolving soup of cells with sporadic coalescence and fragmentation events. Within each cell, the component entities have a strong intra-cell coherence. Between cells, the inter-cell coherence is weak. At time t, we imagine picking an agent i at random – or equivalently, a cell is randomly selected with probability proportional to size. We let s_i be the strength (i.e. size) of the cell to which this agent belongs. With probability ν_{frag}, the coherence of a given cell fragments completely into s_i cells of size one. If it does not fragment, a second cell is randomly selected with probability again proportional to size – or equivalently, another agent j is picked at random. With probability ν_{coal}, the two cells then coalesce, by which we mean that they develop a common "coherence" in terms of their thinking or activities. Analysis of a simple version of this model was completed earlier by d'Hulst and Rodgers [4], and real-world applications have focused on financial markets – however

https://doi.org/10.1017/S0956792515000388 Published online by Cambridge University Press

the derivation below features general values v_{frag} and v_{coal}. The Master Equations are as follows: The equation for the number of cells (i.e. clusters) of strength (i.e. size) s for $s \geqslant 2$ and $s = 1$ are respectively:

$$\frac{\partial n_s}{\partial t} = \frac{v_{\text{coal}}}{N^2} \sum_{k=1}^{s-1} k n_k (s-k) n_{s-k} - \frac{v_{\text{frag}} s n_s}{N} - \frac{2 v_{\text{coal}} s n_s}{N^2} \sum_{k=1}^{\infty} k n_k, \tag{3.1}$$

$$\frac{\partial n_1}{\partial t} = \frac{v_{\text{frag}}}{N} \sum_{k=2}^{\infty} k^2 n_k - \frac{2 v_{\text{coal}} n_1}{N^2} \sum_{k=1}^{\infty} k n_k \quad . \tag{3.2}$$

Here, v_{coal} and v_{frag} are the probabilities per timestep (i.e. rates) of coalescence of two cells, or fragmentation of a cell, respectively. Terms on the right-hand side of equation (3.1) represent all the ways in which n_s can change. Note that the second term on the right-hand side in equation (3.2) includes the coalescence of a 1-agent cell with other 1-agent cells. Strictly, we should remove the self-interaction term since a single agent cannot coalesce with itself, however such a modification can be neglected to a good approximation since n_1 is large. To simplify the limits of the sums, we extend the upper limit to infinity even though $n_s = 0$ for $s > N$. In the steady state

$$s n_s = \frac{v_{\text{coal}}}{(v_{\text{frag}} + 2 v_{\text{coal}}) N} \sum_{k=1}^{s-1} k n_k (s-k) n_{s-k}, \quad s \geqslant 2, \tag{3.3}$$

$$n_1 = \frac{v_{\text{frag}}}{2 v_{\text{coal}}} \sum_{k=2}^{\infty} k^2 n_k \ . \tag{3.4}$$

We now solve these equations using the generating function approach, by considering explicitly the function

$$G[y] = \sum_{k=0}^{\infty} k n_k y^k = n_1 y + \sum_{k=2}^{\infty} k n_k y^k \equiv n_1 y + g[y], \tag{3.5}$$

where y is a parameter and g[y] governs the cell size distribution n_k for $k \geqslant 2$. Multiplying equation (3.3) by y^s and then summing over s from 2 to ∞, yields

$$g[y] = \frac{v_{\text{coal}}}{(v_{\text{frag}} + 2 v_{\text{coal}}) N} G[y]^2, \tag{3.6}$$

i.e.

$$g[y]^2 - \left(\frac{v_{\text{frag}} - 2 v_{\text{coal}}}{v_{\text{coal}}} N - 2 n_1 y \right) g[y] + n_1^2 y^2 = 0 \ . \tag{3.7}$$

From equation (3.5), $g[1] = G[1] - n_1$. Solving for $g[1]$

$$g[1] = \frac{v_{\text{coal}}}{v_{\text{frag}} + 2 v_{\text{coal}}} N, \tag{3.8}$$

hence

$$n_1 = N - g[1] = \frac{v_{\text{frag}} + v_{\text{coal}}}{v_{\text{frag}} + 2 v_{\text{coal}}} N \ . \tag{3.9}$$

https://doi.org/10.1017/S0956792515000388 Published online by Cambridge University Press

Substituting this into equation (3.7) yields

$$g[y]^2 - \left(\frac{v_{\text{frag}} + 2v_{\text{coal}}}{v_{\text{coal}}} N - \frac{2N(v_{\text{frag}} + v_{\text{coal}})}{v_{\text{frag}} + 2v_{\text{coal}}} y \right) g[y] + \frac{(N(v_{\text{frag}} + v_{\text{coal}}))^2}{(v_{\text{frag}} + 2v_{\text{coal}})^2} y^2 = 0 \,. \quad (3.10)$$

We can then go ahead and solve this quadratic for $g[y]$

$$g[y] = \frac{(v_{\text{frag}} + 2v_{\text{coal}})N}{4v_{\text{coal}}} \left(2 - \frac{4(v_{\text{frag}} + v_{\text{coal}})v_{\text{coal}}}{(v_{\text{frag}} + 2v_{\text{coal}})^2} y - 2\sqrt{1 - \frac{4(v_{\text{frag}} + v_{\text{coal}})v_{\text{coal}}}{(v_{\text{frag}} + 2v_{\text{frag}})^2} y} \right), \quad (3.11)$$

which has the expanded form

$$g[y] = \frac{(v_{\text{frag}} + 2v_{\text{coal}})N}{2v_{\text{coal}}} \sum_{k=2}^{\infty} \frac{(2k-3)!!}{(2k)!!} \left(\frac{4(v_{\text{frag}} + v_{\text{coal}})v_{\text{coal}}}{(v_{\text{frag}} + 2v_{\text{coal}})^2} y \right)^k \,. \quad (3.12)$$

If we then go ahead and compare with the definition of $g[y]$ in equation (3.5), this shows that

$$n_s = \frac{(v_{\text{frag}} + 2v_{\text{coal}})N}{2v_{\text{coal}}} \frac{(2s-3)!!}{s(2s)!!} \left(\frac{4(v_{\text{frag}} + v_{\text{coal}})v_{\text{coal}}}{(v_{\text{frag}} + 2v_{\text{coal}})^2} \right)^s . \quad (3.13)$$

Next, we employ Stirling's series

$$ln[s!] = \frac{1}{2} ln[2\pi] + \left(s + \frac{1}{2} \right) ln[s] - s + \frac{1}{12s} - \cdots . \quad (3.14)$$

This means that for $s \geqslant 2$

$$n_s \approx \left(\frac{(v_{\text{frag}} + 2v_{\text{coal}})e^2}{2^{3/2}\sqrt{2\pi} v_{\text{coal}}} \right) \left(\frac{4(v_{\text{frag}} + v_{\text{coal}})v_{\text{coal}}}{(v_{\text{frag}} + 2v_{\text{coal}})^2} \right)^s \frac{(s-1)^{2s-3/2}}{s^{2s+1}} N, \quad (3.15)$$

which in turn implies that

$$n_s \sim \left(\frac{v_{\text{coal}}^{s-1}(v_{\text{frag}} + v_{\text{coal}})^s}{(v_{\text{frag}} + 2v_{\text{coal}})^{2s-1}} \right) s^{-5/2}. \quad (3.16)$$

In the limit $s \gg 1$, this becomes formally equivalent to

$$n_s \sim \exp(-s/s_0) s^{-5/2}, \quad (3.17)$$

where

$$s_0 = -\left[\ln \left(\frac{4(v_{\text{frag}} + v_{\text{coal}})v_{\text{coal}}}{(v_{\text{frag}} + 2v_{\text{coal}})^2} \right) \right]^{-1} \quad (3.18)$$

characterizes the exponential cut-off which appears at very high s [56]. Note that for large cell sizes (i.e. large s such that $s \sim O(N)$), the power law behaviour is masked by the exponential function. Hence, the equilibrium state for the distribution of cell sizes is a power-law with exponent $\alpha \sim 5/2 = 2.5$, together with an exponential cut-off. The fact that the interactions are effectively distance-independent as far as equation (3.1) is concerned, captures the fact that we wish to model human systems, where messages can be transmitted over arbitrary distances (e.g. modern human communications). Our

https://doi.org/10.1017/S0956792515000388 Published online by Cambridge University Press

justification for choosing a cell with a probability which is proportional to its size, is as follows: A cell with more members has more chances of initiating an event. It will also be more likely to find members of another cell more frequently, and hence be able to synchronize with them – thereby synchronizing the two cells. We note that this model also offers, as a by-product, an explanation for Richardson's finding [1] that the distribution of approximately 10^3 gangs in Chicago, and in Manchoukuo in 1935, separately followed a truncated power-law with $\alpha \approx 2.3$.

Following recent empirical findings linking size to lethality [57], we then take a Red cell's strength (size) as proportional to the severity of an event in which it participates. We then assume that the probability that a given Red cell is involved in a given event is set by exogenous factors – in other words, being in the right place at the right time. Therefore, the shape of the distribution of event severities can be mimicked by randomly picking cells and setting the severity equal to the cell strength. As a result, the tail distributions for the event severities and the cell strength will be approximately the same. We have therefore reproduced the observation in Figure 1 that the distribution of severities has an approximate power-law tail $s^{-\alpha}$ with $\alpha \approx 2.5$.

We might wonder if this coalescence–fragmentation model falls down on the basis that an approximate power-law severity distribution apparently exists from the outset of the empirical dataset for each terrorist organization [8] and yet the coalescence–fragmentation process may need time to converge to its steady-state power-law distribution [58]. However, this is not the case. First, the N initial members can be coalescing and fragmenting before any violent event is undertaken – indeed, there are many examples of underground organizations who spend years evolving without any known violent activity. No external event may be observed, but there is still a dynamical network of groups evolving in the background [59]. Any such organization will undoubtedly already have several existing clusters of contacts, hence it is not the case that the distribution has to build up from all isolated agents. A nascent insurgent or cyber group could be created effectively instantly from such an existing structure. Second, numerical simulations show that the fat-tailed distribution does indeed develop very quickly in our model, even if we start with isolated agents. Third, it is highly unlikely that starting from day one of a given organization, all fatal events are recorded in a database. The alternative candidate model proposed in Ref. [7] is a combination of phenomenological broad-brush factors which happen to give a power-law, but without any specific justification for yielding the observed exponent value of 2.5. Instead, the parameters [7] need to be picked in order to obtain the observed power-law exponent value of 2.5. In reality, a continuum of values – including values well away from 2.5 – are just as likely within that model [7]. Moreover, there is little quantitative evidence to support such an alternate mechanism – for example, studies of Provisional Irish Republican Army show that variations in the number of actors can be largely unrelated to variations in the lethality at the level of the entire organization.

4 Attack timing: The dynamical Red Queen model

Following Ref. [28], we now analyse the timing of attacks in terms of a generic arms-race struggle of adaptation and counter-adaptation between Red and Blue. We consider Red (e.g. insurgents) as continually wanting to cause damage to Blue (e.g. kill coalition

https://doi.org/10.1017/S0956792515000388 Published online by Cambridge University Press

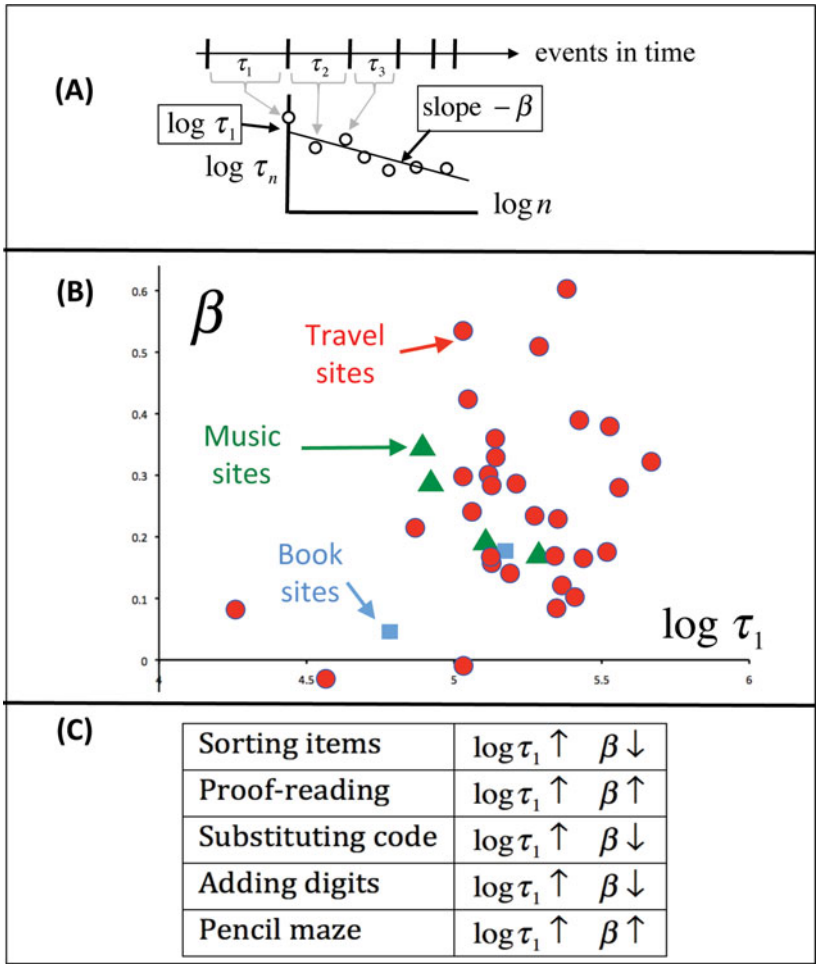

FIGURE 3. Timing of one-sided everyday human activities. There is no Blue opponent to prevent task completion. No clear pattern emerges in (B) or (C) between the progress curve parameters β and τ_1 across individuals. (A) Fitting procedure. Schematic timeline of successive events (i.e. successive completions of task) shown as vertical bars. (B) Results for individuals searching Internet sites. (C) Summary of empirical results in the literature for other individual tasks. Data from Refs. [55] and [54] and adapted from Ref. [47].

military). With all other things being kept equal, then Red would like to complete successful attacks as quickly as possible so that successive successful attacks become more frequent. We therefore analyse the times for successive fatal days for Blue, finding that they follow an approximate power-law progress curve $\tau_n = \tau_1 n^{-\beta}$ [28]. Here, τ_n is the time between the $(n-1)$th and nth fatal day, τ_1 is the time between the first two fatal days, and β describes the subsequent escalation (or de-escalation). A fatal day is one in which Red activity produces at least one death.

We calculated the best-fit power-law progress curve parameters β and τ_1 for each geographical region. Figure 3 shows results from the psychology and organizational literature [54, 55] of what one would expect if the relationship between β and τ_1 for

https://doi.org/10.1017/S0956792515000388 Published online by Cambridge University Press

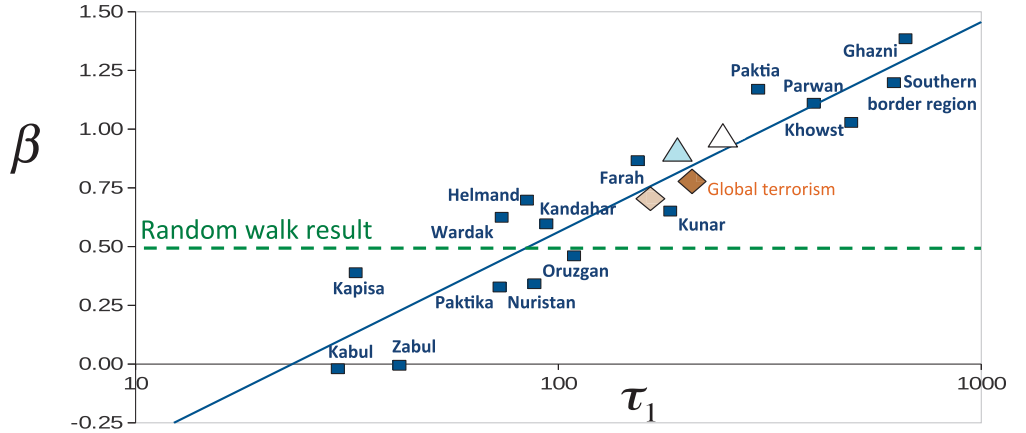

FIGURE 4. Linear dependence emerges between β and log τ_1 for Red attacks in Afghanistan (solid blue line on a semi-log plot). Results are shown for individual Afghanistan provinces (blue squares) for fatal attacks by insurgents (Red) on coalition military (Blue). Green-dashed line shows value $\beta = 0.5$ for random walk (see Figure 5) in which there are no correlations in the dynamics of R. Results for global terrorist attacks also shown (dark diamond is deduced from the best-fit progress curve for global terrorist group activity when averaged over all attacks while the light diamond is an alternative estimate where β and τ_1 are calculated directly by inserting the time intervals between initial attacks into the progress curve formula). Blue triangle shows the results of analysis of Hezbollah suicide attacks, while the white triangle is for suicide attacks within Pakistan (data from cpost.uchicago.edu/). Adapted from Ref. [28].

Red–Blue events followed that of individuals – more specifically, if the dynamics of events emerging from Red–Blue dyads followed the known patterns of behaviour of individuals. In such studies, an individual successfully completes a task that is repeated, just as successive Red attacks imply that Red has managed to carry out a fatal attack against Blue, i.e. Blue has not managed to stop the attack or prevent fatalities. The tasks did not change over time, and hence the situations are akin to Blue not counter-adapting to resist the next attack. Figure 3(B) shows that there is a lack of any monotonic dependence between β and τ_1 for humans completing cyber tasks, specifically the navigation of different websites. In Figure 3(C), individuals repeatedly completed tasks such as proof-reading, solving a puzzle, or purchasing something online. Again, each subject exhibits his/her own β and τ_1. This lack of any generic dependence between β and τ_1 in Figures 3(B) and (C) is no surprise given the heterogeneity of individual humans. By complete contrast, Figure 4 shows that for the recent two-sided insurgent conflict in Afghanistan, an unexpected linear relationship emerges between β and log τ_1 for different geographical regions within the same conflict. This linearity even extends to a specific weapon type i.e. fatalities caused by Improvised Explosive Devices (IEDs) [28].

We now explain this emergence of a so-called progress curve $\tau_n = \tau_1 n^{-\beta}$ for the trend in the timing of attacks leading to Figure 4, using a dynamical version of the Red Queen evolutionary race [28] shown schematically in Figure 5. Further, empirical support is provided by the broad range of insurgent conflicts shown in Figure 6. Our model shown in Figure 5 defines R to be the lead of the Red Queen (e.g. local insurgency) over the Blue King (e.g. coalition military) opponent, i.e. strategic advantage in an arms race.

https://doi.org/10.1017/S0956792515000388 Published online by Cambridge University Press

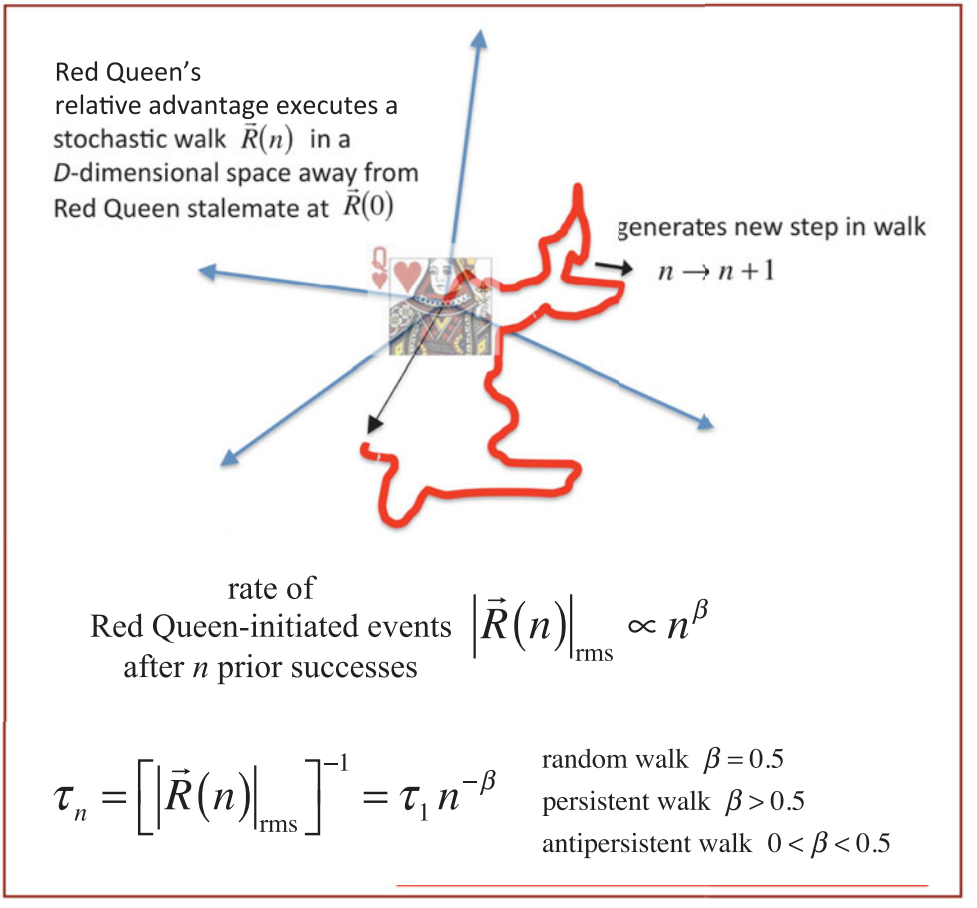

FIGURE 5. Dynamical Red Queen model for the Red–Blue struggle. Red (e.g. insurgent) advantage R is represented as a vector in a multi-dimensional space whose axes may represent technological, psychological, social, cultural or behavioural factors. R follows a stochastic walk in this D-dimensional space. Using known results from statistical physics, exact results can be obtained for β under different conditions of correlation etc. within the walk.

R would more generally be a high-dimensional vector since strategic advantage may involve multiple factors, e.g. training, knowledge of local geography etc. but for simplicity, here we represent it as a scalar and therefore restrict ourselves to a one-dimensional advantage, though we stress that the mathematical nature of multi-dimensional random walks means that our analysis has general validity. In the well-known Red Queen story, she runs as fast as she can in order to stay at the same place, implying that Blue is instantaneously and perfectly counter-adapting to any Red advance, such that they are always neck and neck, i.e. $R = 0$ for all time. Such instantaneous and perfect counter-adaptation is however not possible in practice. Indeed, the complicated adaptation–counter-adaptation dynamics resulting from sporadic changes in the numbers of troops and insurgents, changes in their experience and gathered information, changes in local sentiment or changes in their available weaponry and skills, imply that the temporal

https://doi.org/10.1017/S0956792515000388 Published online by Cambridge University Press

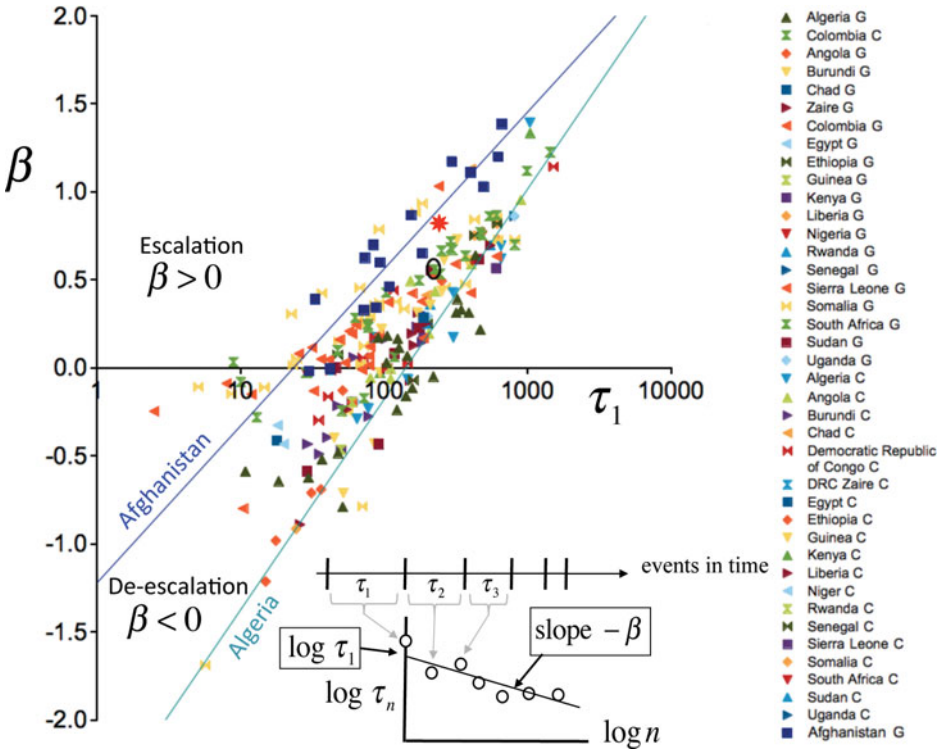

FIGURE 6. Linear dependence between β and $\log \tau_1$ for a wide variety of insurgent conflicts. Various best-fit lines are shown as a guide. For a given symbol (right panel), each data-point shows (τ_1, β) on a semi-log plot, where these (τ_1, β) values are obtained from fitting the trend in inter-event times (lower inset) within a conflict. Red star-shape shows the result from analysis of a dataset containing terrorism attacks aggregated across the globe, and is consistent with the broad mass of geographically-specific points. The black oval ring shows the example of Magdalena, Colombia, and illustrates how places that are geographically distant and hence seemingly unrelated, can have conflicts with very similar dynamics, i.e. they have similar β and $\log \tau_1$ values. These results are insensitive to whether fatal days are counted as (C) days where Red causes civilian (Green) casualties or (G) days where Red causes state security (Blue) casualties. Data-points adapted from Ref. [47].

evolution of R will appear so complex as to be considered random to the eye. This motivates us to model the complex, jerky walk that R undergoes, as a stochastic diffusion process. This means in turn that our statistical results do not require knowledge about the precise mechanism causing a given change in R, nor its value.

A coin-toss process is particularly simple to analyse for R. With an outcome of Tails decreasing R and Heads increasing it, R obeys a random walk. R is Red's lead and hence its instantaneous advantage over Blue, therefore it makes sense to use R as a proxy for the instantaneous rate of fatal days inflicted by Red. As R moves toward zero or becomes negative, the time interval between subsequent fatal days diverges. Provinces in which R is always positive therefore have frequent fatal attacks by Red and show up in Figure 4, while provinces in which R is always negative will not. We expect that any significant changes in R (positive or negative, large or small) occur around days in which Red manages to inflict a fatal attack: Insurgents have by definition become

https://doi.org/10.1017/S0956792515000388 Published online by Cambridge University Press

successful at that moment and so this may stimulate a further increase in their strategic advantage R, while Blue's loss may stimulate an effective counter-adaptation effort and hence reduce R. This means that R is predominantly a function of n (i.e. $R(n)$). A known mathematical result for large n is that the typical magnitude of R after n steps is given by its root-mean-square value $|R(n)|_{\text{rms}} \sim n^{\beta}$, where $\beta = 0.5$ for any diffusion process in which the changes in $R(n)$ are independent and their distribution has finite variance, even if the changes in $R(n)$ do not have the same size. If steps in $R(n)$ have the same size, this result is equivalent to the statement from elementary statistics that the variance of the sum of uncorrelated variables is equal to the sum of the variances. Statistical physics shows that for more general stochastic walks with implicit correlations between changes in $R(n)$, Red's advantage and hence the rate of Red attacks will vary as $|R(n)|_{\text{rms}} \sim n^{\beta}$ with $\beta \neq 0.5$. The time between attacks will hence vary as $|R(n)|^{-1}_{\text{rms}} \sim n^{-\beta}$. By definition this is τ_n.

Therefore, we have derived mathematically the observed empirical result that $\tau_n \propto n^{-\beta}$ and hence $\tau_n = \tau_1 n^{-\beta}$. For a wide range of possible correlations within $R(n)$, it is known that $0 < \beta < 1.5$ in agreement with Figures 4 and 6. If Blue's counter-adaptation is completely absent or inadequate, R persistently increases at every step n and hence $|R(n)|_{\text{rms}} \sim n$ meaning that $\beta \approx 1$. This is analogous to Red moving forward at constant velocity while Blue is left stuck at the starting line. If Red gains momentum, R may even start accelerating and hence $\beta > 1$ as observed for a few points in Figures 4 and 6. Effective Blue counter-adaptation to each Red advance means, by contrast, that R stays close to zero: Therefore, $|R(n)|_{\text{rms}}$ will be of order 1 (i.e. n^0) and hence $\beta \approx 0$. It is only in the idealized – and highly unrealistic – case where Blue's counter-adaptation is instantaneous and perfect, that R will always be exactly zero. Similarly, it is only if Blue proactively produces its own advances that R could become permanently negative and therefore that geographical area has no attacks.

The unweighted linear least-squares approach used to fit the trend in $\log \tau_n$ versus $\log n$ for each point in Figures 4 and 6, provides an unbiased best estimate in the limit that the residuals approach statistical i.i.d. status (independent and identically distributed). This does indeed turn out to be a good approximation in our study, allowing us to propose a failure process to model the dynamics leading up to each attack. Specifically, our empirical analysis has shown that the error (i.e. fluctuations) in the underlying τ_n values have a crudely multiplicative form, like a failure process, implying that

$$\tau_n = \mathbf{X}\tau_1 n^{-\beta}, \tag{4.1}$$

where $\mathbf{X}$ is a multiplicative noise process of the form $\mathbf{X} = \prod_y^Y (1 + \epsilon_y)$ and where $\{\epsilon_y\}$ are drawn from a random distribution with finite variance. Each fatal Red attack can therefore be seen as a failure process in which a set of Y processes need to go "wrong" in order that Red can create its next fatal attack. Taking the logarithm of both sides yields

$$\log \tau_n = \sum_y^Y \{\log (1 + \epsilon_y)\} + \log \tau_1 - \beta \log n. \tag{4.2}$$

https://doi.org/10.1017/S0956792515000388 Published online by Cambridge University Press

Using the well-known result that $\log(1+\epsilon_y) \approx \epsilon_y$ when $\epsilon_y \ll 1$ yields

$$\log \tau_n = \sum_{y}^{Y} \epsilon_y + \log \tau_1 - \beta \log n, \tag{4.3}$$

meaning that a plot of $\log \tau_n$ versus $\log n$ will produce a scatter of points around the straight line

$$\log \tau_n = \log \tau_1 - \beta \log n, \tag{4.4}$$

with residuals that are sums of $\{\epsilon_y\}$. We have verified empirically that the distribution of the residuals is approximately Gaussian with no serial correlations, consistent with such i.i.d. variables and hence supporting our identification of a progress curve to describe the trend in attack timings in Figures 4 and 6.

Using this dynamical Red Queen model, we can therefore interpret and compare the entire spectrum of observed β values for different provinces, and also different terrorism domains, in an intuitive and unified way using language concerning the relative advantage between Red and Blue. Most importantly, this broad-brush Red Queen model does not require knowledge of specific adaptation or counter-adaptation mechanisms, and therefore avoids issues such as changes in technology, learning, skill-set, or insurgent membership (i.e. composition, numbers or numbers of cells). It also removed any need to know the hearts and minds of local residents. Instead, a change in Red's lead R might result from a conscious or unconscious adaptation by Red, or by Blue, or both – for example, there may be an increase in Red numbers because of a conscious recruitment campaign or simply due to bad press involving Blue's activity. Likewise, R may change due to a surge in Blue's numbers or strength, or a change in its tactics or defences. It does not matter: The precise cause for changes in R does not affect the validity of our theory. The fact that the relationships in Figures 4 and 6 are linear, suggests an intriguing coupling between the way in which Red and Blue are fighting in each region. If the dynamics were completely independent within each separate geographic area in a given conflict, the corresponding (β, τ_1) points could in principle lie scattered anywhere in the plane in Figures 4 and 6. If they were identical, they would lie on top of each other. However, the fact that they follow a linear relationship, suggests the existence of a weak coupling between them. The precise origin and nature of such a coupling awaits a future detailed mathematical model.

Figure 7 shows this same analysis applied to the timing of cyber attacks [60]. We extracted the data for the cyber-attacks from the February 2013 report by MANDIANT on cyber attacks by a suspected Chinese group (Red) against national infrastructure sectors (Blue). As confirmed by Figure 7(A), no pattern appears when the timing of the attacks is randomized – yet a clear linear relationship emerges for the actual attack data, just as in Figures 4 and 6 for insurgent and terrorist attacks. This suggests that the pattern that we observe in the timing of attacks and their potential escalation and de-escalation is indeed general to real-world insurgencies, to terrorism campaigns, and to cyber-terrorism. We await data on future cyber-attacks to further test this finding concerning the timing pattern, as well as data on the severity of cyber-attacks to compare with Figure 1.

https://doi.org/10.1017/S0956792515000388 Published online by Cambridge University Press

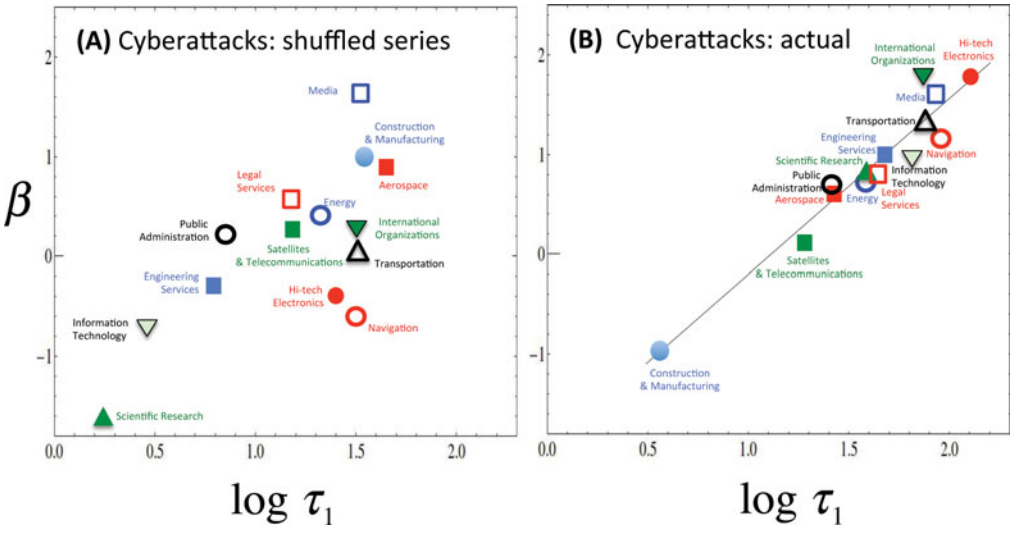

FIGURE 7. Results from analysis of the timing of cyber-attacks by a suspected Chinese group (Red) against national infrastructure sectors (Blue). Underlying data taken from the February 2013 report of MANDIANT [60]. The analysis performed on the timing of attacks and the resulting plot are exactly the same as Figures 3, 4 and 6. Each point denotes a unique sector of national cyber-infrastructure. (A) Results for randomized attack times. (B) Results for actual attack times. Data-points taken from Ref. [47].

5 Conclusions

We have been able to present a modelling approach to human conflict in two largely separate stages for the severity and timing respectively of attacks. This is justified because of the lack of strong correlations between the severity of attacks and their timing. For the attack severity, we provided a mathematical model of Red's internal dynamics comprising dynamically evolving cells in a loose and sporadically-changing structure. For the attack timing, our dynamical Red Queen theory described the timing of fatal events [28].

Various practical implications follow from our work. Let us suppose that violent events begin to emerge in a given region, and that they appear to follow a crude power-law distribution with slope similar to 2.5. The inference is then that Red operates with a similar delocalized cluster structure to our model. Even in the absence of any observed events, the generality of the results in Figure 1 suggests that the distribution of any future events will follow a similar form. Using this power-law form, one can calculate the expected number of casualties in a future attack to be approximately $[(\alpha-1)/(\alpha-2)]s_{\min}$ with $s_{\min}$ being the cut-off in the maximum-likelihood fit. Another consequence of our model and in particular the coalescence–fragmentation process, is that a lone-wolf actor is only truly alone for short periods of time. This is again consistent with recent field studies, and the equations can be used to estimate how long ago contact was made with other Red clusters. Turning to the timing of attacks, let us suppose some sporadic attacks have been observed in a given location or sector in the real or online world. If successive time-intervals between attacks follow the trend $\tau_1 n^{-\beta}$, the suggestion is that they are all generated by a single Red–Blue process. Assuming Red dominates the Red–Blue dynamic,

https://doi.org/10.1017/S0956792515000388 Published online by Cambridge University Press

this implies a single attacking Red entity. Suppose that attacks then emerge in different locations or sectors: If an approximate linear relationship then emerges between β and τ_1 as in Figure 4, this suggests that the same Red is operating in these different places.

Our final comment concerns a comparison to results for street gangs and cyber-gangs, specifically the empirical distributions for Long Beach street gang sizes and online guild sizes for World of Warcraft that we published in Ref. [35]. We had found that the empirical distributions were not power-law like – however, this difference can be explained by the fact that our analysis had considered the time-averaged membership of online guilds and gangs, as well as street gangs, as opposed to the number of objects who happen to be coordinated (e.g. online, or on the street) at any given time as in the present paper. The latter is likely to vary rapidly and spontaneously every day as members come online or onto the street, however the underlying membership would be expected to change more slowly over timescales of months. In addition, when individuals leave a street gang or an online guild, it is unlikely that this happens because the entire gang or guild is disbanding – hence, the fragmentation process in our model would not be applicable. Instead, it is known that fragmentation processes involving the partial dismantling of a large cell into just a few randomly chosen splinter-cells tend to generate non-power-law distributions, as indeed we observed for street gangs and online guilds in Ref. [35].

Acknowledgement

We are extremely grateful to the many collaborators that have made many of these results possible, including Pablo Medina, Mike Spagat, John Horgan, Paul Gill, Brian Tivnan, Pak Ming Hui, Spencer Carran, Juan Camilo Bohorquez, Roberto Zarama, Guannan Zhao, Pedro Manrique and Hong Qi and all other co-authors on the papers that we cite and review. The views and conclusions contained in this paper are those of the authors and should not be interpreted as representing the official policies, either expressed or implied, of any of the above named organizations, to include the U.S. government.

References

[1] Richardson, L. F. (1960) Statistics of deadly quarrels (Boxwood, Pittsburgh).
[2] Lanchester, F. W. (1956) Mathematics in warfare. In: J. R. Newman, Simon & Schuster (editors), *The World of Mathematics*, Vol. 4, pp. 2138.
[3] Ispolatov, I., Krapivsky, P. L. & Redner, S. (1996) War: The dynamics of vicious civilizations. *Phys. Rev. E* **54**, 1274.
[4] D'Hulst, R. & Rodgers, G. J. (2000) Exact solution of a model for crowding and information transmission in financial markets. *Int. J. Theor. Appl. Finance* **3**, 609.
[5] Eguiluz, V. & Zimmermann, M. (2000) Transmission of information and herd behavior: An application to financial markets. *Phys. Rev. Lett.* **85**, 5659.
[6] Galam, S. (2002) Minority opinion spreading in random geometry. *Eur. Phys. J. B* **25**, 403.
[7] Clauset, A., Young, M. & Gleditsch, K. S. (2007) On the Frequency of Severe Terrorist Events. *J. Conflict Resolution* **51**, 1.
[8] Clauset, A. & Gleditsch, K. S. (2011) The developmental dynamics of terrorist organizations. Preprint, http://arxiv.org/abs/0906.3287 PLOS ONE 7(11): e48633 (2012).
[9] Galam, S., & Mauger, A. (2003) On reducing terrorism power: A hint from physics. *Physica A* **323**, 695.

[10] Lim, M., Metzler, R. & Bar-Yam, Y. (2007) Global pattern formation and ethnic/cultural violence. *Science* **317**, 1540.
[11] Couzin, I. D. (2006) Behavioral ecology: Social organization in fission–fusion societies. *Curr. Biol.* **16**, R170.
[12] Braithwaite, A. & Johnson, S. D. (2012) Space-time modeling of insurgency and counter-insurgency in Iraq. *J. Quant. Criminology* **28**, 31.
[13] Bowers, K. J. & Johnson, S. D. (2014) Crime mapping as a tool for security and crime prevention. In: *The Handbook of Security*, Palgrave Macmillan, London.
[14] Woodworth, J. T., Mohler, G. O., Bertozzi, A. L. & Brantingham, P. J. (2014) Nonlocal crime density estimation incorporating housing information. *Phil. Trans. Roy. Soc. A* **372**, 20130403.
[15] Zipkin, J., Short, M. B., Bertozzi, A. L. (2014) Cops on the dots in a mathematical model of urban crime and police response. *Discrete Continuous Dyn. Syst. B* **19**, 1479.
[16] Gambetta, D. (2009) *Codes of the Underworld: How Criminals Communicate*, Princeton University Press. Princeton, NJ, USA.
[17] Robb, J. (2007) *Brave New War: The Next Stage of Terrorism and the End of Globalization*, Wiley. Hoboken, NJ, USA.
[18] Kenney, M. (2007) *From Pablo to Osama: Trafficking and Terrorist Networks, Government Bureaucracies, and Competitive Adaptation*, Pennsylvania State University Press. University Park, PA, USA.
[19] Kilcullen, D. (2009) *The Accidental Guerrilla: Fighting Small Wars in the Midst of a Big One*, Oxford University Press, Oxford.
[20] Kalyvas, S. N. (2006) *The Logic of Violence in Civil War*, Cambridge University Press, Cambridge.
[21] Buhaug, H., Cederman, L. E. & Gleditsch, K. S. (2013) *Grievances and Inequality in Civil Wars*, Cambridge University Press, Cambridge.
[22] Johnson, D. D. P. & Tierney, D. (2011) The Rubicon theory of war: How the path to conflict reaches the point of no return. *Int. Secur.* **36**, 7.
[23] Bohannon, J. (2011) Counting the dead in Afghanistan. *Science*. **331**, 1256.
[24] Caro, T. (2005) *Antipredator Defenses in Birds and Mammals*, University of Chicago Press. Chicago, IL, USA.
[25] Horgan, J. (2005) *Psychology of Terrorism*, Routledge, Abingdon.
[26] McCulloh, I. A., Carley, K. M. & Webb, M. (2007) Social network monitoring of Al-Qaeda. *Netw. Sci.* **1**, 25.
[27] Johnson, N., Jefferies, P. & Hui, P. (2003) *Financial Market Complexity*, Oxford University Press, Oxford.
[28] Johnson, N., Carran, S., Botner, J., Fontaine, K., Laxague, N., Nuetzel, P., Turnley, J. & Tivnan, B. (2011) Pattern in escalations in insurgent and terrorist activity. *Science* **333**, 81.
[29] Bohorquez, J. C., Gourley, S., Dixon, A., Spagat, M. & Johnson, N. (2009) Common ecology quantifies human insurgency. *Nature* **462**, 911.
[30] Johnson, N. F., Manrique, P. & Hui, P. M. (2013) Heterogeneity in conflict dynamics. *J. Stat. Phys.* DOI 10.1007/s10955-013-0706-z. Vol 151, p. 395 (2013).
[31] For full details, see http://mathematicsofwar.com/
[32] Zhao, Z., Bohorquez, J. C., Dixon, A. & Johnson, N. F. (2009) Anomalously slow attrition times for asymmetric populations with internal group dynamics. *Phys. Rev. Lett.* **103**, 148701.
[33] Ruszczycki, B., Zhao, Z., Burnett, B. & Johnson, N. F. (2009) Relating the microscopic rules in coalescence-fragmentation models to the cluster-size distribution. *Eur. Phys. J.* **72**, 289.
[34] Johnson, N. F., Ashkenazi, J., Zhao, Z. & Quiroga, L. (2011) Equivalent dynamical complexity in a many-body quantum and collective human system. *AIP Adv.* **1**, 012114.
[35] Johnson, N. F., Xu, C., Zhao, Z., Ducheneaut, N., Yee, N., Tita, G. & Hui, P. M. (2009) Human group formation in online guilds and offline gangs driven by a common team. *Phys. Rev. E* **79**, 066117.

[36] Dixon, A., Zhao, Z., Bohorquez, J. C., Denney, R. & Johnson, N. (2010) Statistical physics and modern human warfare. In: G. Naldi *et al.* (editors), *Mathematical Modeling of Collective Behavior in Socio-Economic and Life Sciences*, Birkhauser, Boston, MA, p. 365.
[37] Zhao, Z., Kirou, A., Ruszczycki, B. & Johnson, N. F. (2009) Dynamical clustering as generator of complex system dynamics. *Math. Models Methods Appl. Sci.* **19**, 1539.
[38] Zhao, Z., Calderon, J. P., Xu, C., Zhao, G., Fenn, D., Sornette, D., Crane, R., Hui, P. M. & Johnson, N. F. (2010) Effect of social group dynamics on contagion. *Phys. Rev. E* **81**, 056107.
[39] Johnson, N. (2008) Mathematics, physics and crime. *Policing* **2**, 160.
[40] Johnson, N. F. (November 2006) The Mother (Nature) of All Wars: Conflict, global terrorism and complexity science. APS News.
[41] Johnson, N. F. (2008) Complexity in human conflict. In: D. Helbing (editor), *Managing Complexity: Insights, Concepts, Applications*, Springer, Berlin, p. 303.
[42] Johnson, N., Spagat, M., Restrepo, J., Bohorquez, J., Suarez, N., Restrepo, E. & Zarama, R. (2005) From old wars to new wars and global terrorism. e-print arXiv:physics/0506213.
[43] Johnson, N. F., Spagat, M., Restrepo, J. A., Becerra, O., Bohorquez, J. C., Suarez, N., Restrepo, E. M. & Zarama, R. (2006) Universal patterns underlying ongoing wars and terrorism. e-print arXiv:physics/0605035.
[44] Bouchaud, J. P. & Potters, M. (2004) *Theory of Financial Risk and Derivative Pricing: From Statistical Physics to Risk Management*, Cambridge University Press, Cambridge.
[45] Mantegna, R. N. & Stanley, H. E. (1995) Scaling behaviour in the dynamics of an economic index. *Nature* **376**, 46.
[46] Johnson, N. F., Restrepo, E. M. & Johnson, D. E. (2015) Modeling human conflict and terrorism across geographic scales. In: B. Gonzalves (editor), *Social Phenomena: From Data to Models*, Springer, pp. 3–25. New York, USA.
[47] Johnson, N. F., Medina, P., Zhao, G., Messinger, D. S., Horgan, J., Gill, P., Bohorquez, J. C., Mattson, W., Gangi, D., Qi, H., Manrique, P., Velasquez, N., Morgenstern, A., Restrepo, E., Johnson, N., Spagat, M. & Zarama, R. (2013) Simple mathematical law benchmarks human confrontations. *Sci. Rep.* **3**, 3463.
[48] Restrepo, J., Spagat, M. & Vargas, J. (2006) The severity of the colombian conflict: Cross-country datasets versus new micro data. *J. Peace Res.* **43**, 99.
[49] Kappler, K. E. & Kaltenbrunner, A. (2012) The power laws of violence against women: Rescaling research and policies. *PLoS ONE* **7**, e40289.
[50] Epstein, J. (1997) *Nonlinear Dynamics, Mathematical Biology and Social Sciences*, Addison-Wesley, Reading.
[51] MacKay, N. J. (2006) Lanchester combat models. *Math. Today: Bull. Inst. Math. Appl.* **42**, 170.
[52] Felson, M. (2007) *Crime and Nature*, Sage Publications. Thousand Oaks, CA, USA.
[53] Hedstrom, P. & Ylikoski, P. (2010) Causal mechanisms in the social sciences. *Annu. Rev. Sociol.* **36**, 49.
[54] Crossman, E. R. F. W. (1959) A theory of the acquisition of speed-skill. *Ergonomics* **2**, 153.
[55] Johnson, E., Bellman, S. & Lohse, G. L. (2003) Cognitive Lock-In and the power law of practice. *J. Mark.* **67**, 62.
[56] Clauset, A., Shalizi, C. & Newman, M. E. J. (2007) Power-law distributions in empirical data. *SIAM Rev.* **51**, 661.
[57] Asal, V. & Rethemeyer, R. K. (2008) The nature of the beast: Organizational structures and the lethality of terrorist attacks. *J. Politics* **70**, 437.
[58] Clauset, A. & Wiegel, F. W. (2010) A generalized aggregation-disintegration model for the frequency of severe terrorist attacks. *J. Conflict Resolution* **54**, 179.
[59] Humphries, D. A. & Driver, P. M. (1970) Protean defence by prey animals. *Oecologia* **5**, 285.
[60] Exposing One of China's Cyber Espionage Units, Mandiant. (2013). Accessed 19 march 2013. URL: intelreport.mandiant.com/Mandiant_APT1_Report.pdf